

Preliminary Modeling, Testing and Analysis of a Gas Tankless Water Heater

Conference Paper - 1002

May 2008

Jay Burch (NREL), Jeff Thornton (Thermal Energy Systems Specialists), Marc Hoeschele and Dave Springer (Davis Energy Group), Armin Rudd (BSC)

Abstract:

Tankless water heaters offer significant energy savings over conventional storage-tank water heaters, because thermal losses to the environment are much less. Although standard test results are available to compare tankless heaters with storage tank heaters, actual savings depend on the draw details because energy to heat up the internal mass depends on the time since the last draw. To allow accurate efficiency estimates under any assumed draw pattern, a one-node model with heat exchanger mass is posed here. Key model parameters were determined from test data. Burner efficiency showed inconsistency between the two data sets analyzed. Model calculations show that efficiency with a realistic draw pattern is ~8% lower than that resulting from using only large ~40 liter draws, as specified in standard water-heater tests. The model is also used to indicate that adding a small tank controlled by the tankless heater ameliorates unacceptable oscillations that tankless with feedback control can experience with pre-heated water too hot for the minimum burner setting. The added tank also eliminates problematic low-flow cut-out and hot-water-delay, but it will slightly decrease efficiency. Future work includes model refinements and developing optimal protocols for parameter extraction.

PRELIMINARY MODELING, TESTING AND ANALYSIS OF A GAS TANKLESS WATER HEATER

Jay Burch
National Renewable Energy Laboratory
1617 Cole Blvd.; Golden, CO 80401
E-mail: jay_burch@nrel.gov

Marc Hoeschele and Dave Springer
Davis Energy Group

Armin Rudd
Building Science Corporation

Jeff Thornton
Thermal Energy Systems Specialists

ABSTRACT

Tankless water heaters offer significant energy savings over conventional storage-tank water heaters, because thermal losses to the environment are much less. Although standard test results are available to compare tankless heaters with storage tank heaters, actual savings depend on the draw details because energy to heat up the internal mass depends on the time since the last draw. To allow accurate efficiency estimates under any assumed draw pattern, a one-node model with heat exchanger mass is posed here. Key model parameters were determined from test data. Burner efficiency showed inconsistency between the two data sets analyzed. Model calculations show that efficiency with a realistic draw pattern is ~8% lower than that resulting from using only large ~40 liter draws, as specified in standard water-heater tests. The model is also used to indicate that adding a small tank controlled by the tankless heater ameliorates unacceptable oscillations that tankless with feedback control can experience with pre-heated water too hot for the minimum burner setting. The added tank also eliminates problematic low-flow cut-out and hot-water-delay, but it will slightly decrease efficiency. Future work includes model refinements and developing optimal protocols for parameter extraction.

1. INTRODUCTION

Tankless water heaters (TWH) save energy primarily by eliminating the energy losses associated with a storage tank, and their market share is increasing (1). Pros and cons of TWHs generally are shown in Table 1, with energy savings (see Table 2) probably the key factor driving increased interest. Savings are most often estimated using published energy factors [EF \equiv $Q_{to\ load}/Q_{in}$], which are measured at 64 gal/day usage with 6 draws of 10.6 gal each (2). Although reasonable for storage tank water heaters, using a few large draws unrealistically minimizes the impact of cycling of the heat exchanger mass with TWH. Each cool-down of that mass wastes a certain amount energy to the environment,

and the more draws/per day there are, the more waste and inefficiency there is. Using an accurate simulation model will permit efficiency estimation for *any* draw pattern (e.g., that deemed best by a standards-making body). To make the simulation model accurate for a given unit while keeping the model simple, key model parameters should be derived from simple tests. In this paper, a model is proposed whose key parameters can be determined by tests which could be executed in under an hour.

TABLE 1. PROS AND CONS OF TANKLESS

Pro/Advantages	Con/Disadvantages
Energy savings	Higher first cost/maintenance
Endless hot water	Increased hot water usage ¹
Compact/space savings	Imperfect temperature control
Low weight	Minimum flow rate to turn on
Builder- & DIY-friendly	Limited capacity/hi-flow limit
Calif. Title 24 Credits	Delays in hot water delivery

1. No hard data exists to support this reasonable conjecture.

There are two types of TWHs: gas and electric. For whole-house applications, systems are predominantly gas because of the high power demand. For example demand is more than 200 kBtu/hr (30kW) at 6 gpm with a 70 °F temperature rise. Gas TWH have somewhat larger savings potential than electric TWH do, because conventional gas tanks with their central flue design are more inefficient to begin with (EF ~0.58) compared to electric storage-tank water heaters (EF ~0.92). Although all the modeling introduced here applies equally to gas or electric systems with minor parameter changes, gas dominates the whole-house tankless market (1) and is of primary interest here.

TABLE 2. WH ENERGY FACTORS AND SAVINGS

Water Heater	Energy factor ¹	Savings ²
Gas storage tank	0.55-.63; >.88 ³	-
Gas tankless	0.69-.83; >.95 ³	~25-45%

1) Data taken from (2), except for condensing units.

2) % savings = (EF_{tnkls} - EF_{tnk})/EF_{tnk}

3. Emerging condensing gas units, not yet listed in (2).

Savings from TWH are most often inferred from standard water heater tests (2). Typical EFs and estimation of savings are shown in Table 2. The test procedure specifies six equal draws of ~10.6 gal each, one hour apart, as in Fig. 1. The issue here is not with the total daily draw volume; 64 gal/day is a reasonable average. However, realistic usage invariably shows frequent small sink draws, as also shown in Fig. 1. This is of little consequence for storage water heaters, where the outlet temperature is mostly independent of draw volume, flow rate, and time (short of runout); but it is critical for tankless.

To analyze tankless efficiency, it is useful to define an efficiency for each draw:

$$\eta_{\text{draw}} = Q_{\text{out}}/Q_{\text{in}} = [\int_{\text{draw}} dt (m_{\text{dot}} c_p (T_{\text{out}} - T_{\text{in}}))] / \{ \int_{\text{draw}} dt Q_{\text{dot}, \text{in}} \} \quad (1)$$

(see Nomenclature, Section 7, for definition of terms). In the standard test (2), η_{draw} and the resulting EF are close to the burner efficiency η_{burn} , as the energy to charge up the heat exchanger is small compared to the draw energy. However, η_{draw} is much lower than the EF for small draws, as shown in Fig. 2 (3). Thus, actual long-term efficiency of a TWH depends on the details of the draw schedule and will be generally lower than EFs published at (2). Actual draw patterns are very complex, and no draw pattern is universally accepted; each standards-making body or study will want to make their own assumptions. In this paper, a model is proposed that will allow reasonably-accurate calculation of efficiency for *any* assumed draw pattern.

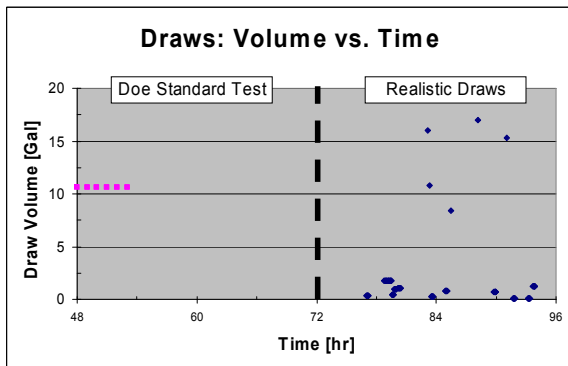


Fig. 1. The standard test draw profile (left side), contrasted to a more realistic draw pattern (right side).

An empirical approach to estimating efficiency with realistic draws was used in a previous study (3). In that work, the efficiencies of individual hot water draws were taken with set delay times of 1, 5, 10, and 45 minutes (delay time is the time since the previous draw). In Fig. 2, the upper line characterizes efficiency of a “hot” tankless unit (recent draw) and the lower line applies to a “cold” unit (no recent draw). The draw efficiencies were combined with binned draw distribution taken from a monitored home. The

resulting efficiency was 0.73, versus 0.81 from EF in (2). Realistic draws lowered efficiency on the order of 10%. Tankless models developed previously have varied in structure and capability. A massless model assuming ideal continuous control, constant efficiency, and a maximum power input has been available for many years in the public domain (4). Although adequate for general studies, this model is moot on most details of tankless operation. It cannot address variations in efficiency with draw patterns or temperature control issues. On the other end of the spectrum, detailed models that include combustion and flow modeling would be used by product developers. This type of model would provide accurate calculations, but it is quite unwieldy and not suitable for automated calibration to data or for annual simulations. The model posed here is at an intermediate level: simple but sufficiently complex to accommodate mass effects that impact efficiency.

2. TANKLESS MODEL

A TWH is relatively complex compared to a conventional storage-tank heater. The auxiliary power input rate must modulate to produce a reasonably-constant outlet temperature, even in the face of rapidly-varying draw flow rates. Microprocessors are often used with PID control; older units had simple pressure controls and temperature control was not as good. In contrast, storage water heaters have simple on-off controls and automatically produce reasonably constant outlet temperature until runout occurs. Gas input rates vary both in discrete steps and continuously, depending on the manufacturer and model. A bypass valve is used to improve temperature control under certain conditions. A flow limiting valve is included on some models to limit temperature sag below setpoint. Table 3 shows some of the key technical parameters for TWH generally.

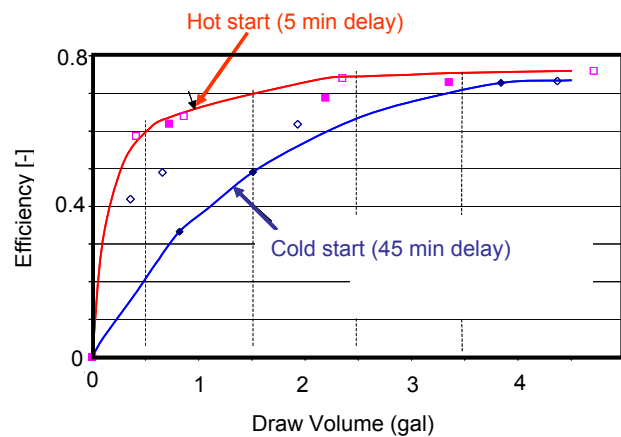


Fig. 2. Draw efficiency versus the volume of the draw, for 5 min. and 45 min. delay. Adapted from (3).

TABLE 3. KEY GAS TANKLESS PARAMETERS

Parameter	Range ¹	Tested unit ²
Energy factor	0.69-0.84; >0.95 ³	0.81
Conversion efficiency	0.79-0.85; >0.95 ³	NK ⁴
Maximum power	100-200 kBtu/hr	140 kBtu/hr
Minimum flow ⁵	0.5 – 0.8 gpm ⁵	0.75 gpm
Power modulation ⁶	Discrete and cont.	NM ⁴ ; discrete?
Burner/bypass control	Varies	NM ⁴
Effective deadband	Varies	NM ⁴
Water content	.1-1 gal	NM ⁴
Delay in firing	3-10 sec	~5 sec.
Electric parasitic power (off/on) ⁷	1-10 W//30-100 W	5 W//75 W

1. Data mostly from the tankless rating directory in (2).
2. Manufacturer's data; the unit is currently not listed at (2).
3. For electric: $\eta_{\text{burn}} \equiv 1$, and $EF > .99$. For gas, condensing units with $EF > 0.95$ are recently available.
4. NM = Not measured, NK = not known
5. Applies to all gas and electric/discrete units.
6. Some TWH can vary continuously; others have discrete levels only.
7. Electrical power includes microprocessor, controls/sensors, and fan(s), in both on and off states

The model used here is shown in Fig. 3. It consists of a single lumped node for the heat exchanger and water mass, with coupling to T_{env} , draw loss, and gas input. In reality, there is a temperature gradient along the heat exchanger, and higher order models will likely be needed ultimately. An energy balance on the mass node yields the equation:

$$C \, dT/dt = \eta Q_{\text{dot,gas}} - \dot{m}_{\text{dot}} c_p (T - T_{\text{in}}) - UA(T - T_{\text{env}}) \quad (1)$$

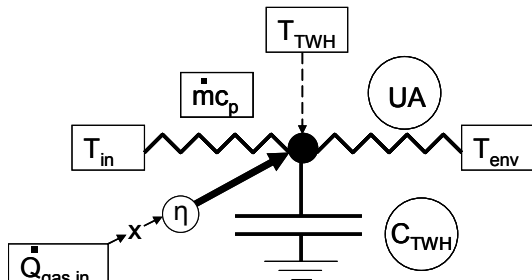


Fig. 3. Tankless thermal circuit model. Variables in boxes are measured; parameters in circles are to be determined.

The modeling framework TRNSYS was used (4). Documentation of the tankless model can be found at (5). Constraints imposed on the model include: i) there is a user-specified delay after the draw starts before the burner ignites (~5 secs, for establishing fan flow and safety interlocks); ii) there is a minimum flow rate to actuate the burner (0.5-0.8 gpm); iii) there are minimum and maximum Q_{dot} (for gas, $Q_{\text{dot,min}}$ is typically 10% to 20% of $Q_{\text{dot,max}}$). The time step is subdivided into constant- Q_{dot} portions as needed whenever

controls change burner setting, and averages are computed over the time-step.

Q_{dot} can be *continuous* or *discrete*. Controls for the discrete case use a “feedback + deadband” approach. At start of a time-step, if $\dot{m}_{\text{dot}} > \dot{m}_{\text{dot,min}}$, the burner was previously off, and ($T_{\text{out}} < T_{\text{set}}$), Q_{dot} is set to $Q_{\text{dot,max}}$. If ($T_{\text{out}} > T_{\text{set}}$) occurs during the time-step, the burner is re-set downward one step. If ($T_{\text{out}} > T_{\text{set}}$) occurs at $Q_{\text{dot,min}}$, then the burner is turned off. Then, when ($T_{\text{out}} < T_{\text{set}} - T_{\text{dband}}$), the burner start cycle is re-initiated, with the concomitant delay. This will lead to large oscillations when T_{in} is too high, as described in Section 5 and in (3). TWH with feed-forward control anticipate and avoid this issue. Feed-forward units are not yet modeled.

New models should first be validated analytically insofar as possible. Fig. 4 shows the model response to varying flow rate, to compare to expectation. In region 1, there is decay from a previous firing toward T_{env} . In region 2, a draw is initiated with $\dot{m}_{\text{dot}} < \dot{m}_{\text{dot,min}}$, and the unit does not fire. In regions 3 and 5, flow rate varies, with $\dot{m}_{\text{dot}} > \dot{m}_{\text{dot,min}}$, and T_{out} is maintained at T_{set} . In region 4, the power needed to reach setpoint is above $Q_{\text{dot,gas,max}}$, and T_{out} sags down below T_{set} . The flow in region 6 is too low to fire the burner, and the cold mains water flowing through lowers T_{out} below T_{amb} . This leads to a rise in T_{out} toward T_{amb} in region 7. All this behaviour (and the time constants) is as expected.

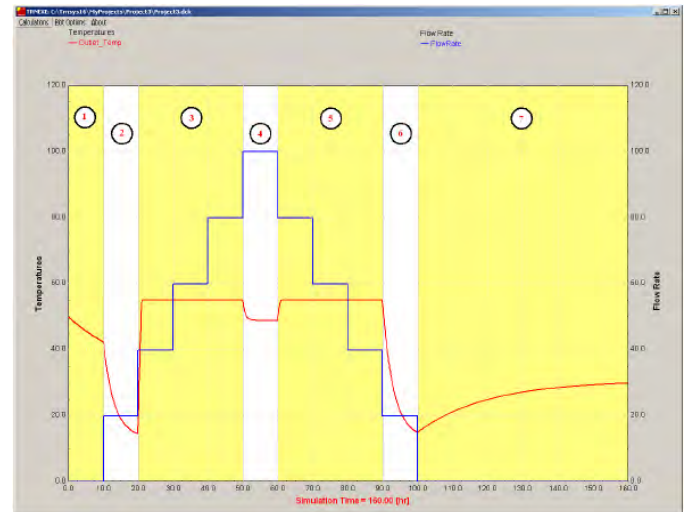


Fig. 4. Model response to varying flow rates. The red line is T_{out} , and the blue line is $\dot{m}_{\text{dot,in}}$.

3. GAS TANKLESS DATA

Data taken in a previous study was used (3). In that study, a gas TWH was set up and instrumented as in Fig. 5. Table 4 shows the monitoring points and assumed uncertainties. The data time step was either 5 sec or 1 sec. The test space was

unconditioned; T_{env} was not measured, but could be estimated as T_{out} at the start of a those draws taken at least 45 min after the previous draw. Flow rates were measured with pulse-initiating meters, introducing noise in rates for small draws. A floating average is used to smooth the pulse-output channels. Electrical consumption of the fan and control system were not continuously measured, but one-time measurements were taken. The logger was activated only when a draw was taken, as the goal was to measure η_{draw} . Unfortunately, this created “holes” which need to be filled for TRNSYS use (although gas and water flow rates were known to be zero during the hole). Filled data were not used in the regression of parameters.

TABLE 4. DATA CHANNELS AND SPECIFICATIONS

Variable ¹	Uncertainty
Water inlet ²	1.0 °F (0.5 °C)
Water outlet ²	1.0 °F (0.5 °C)
Water flow rate ³	(488.6 pulses/gal); 2%
Gas flow rate ⁴	(0.051 ft ³ /pulse); 3%

1. Data were logged with a Data Electronic s DT-50 logger.
2. Measured with Gordon Type T immersion thermocouples.
3. Measured with an Onicon F1300 flow meter
4. Measured with an Equimeter S-275P gas meter; error includes uncertainty in heat content of the gas.

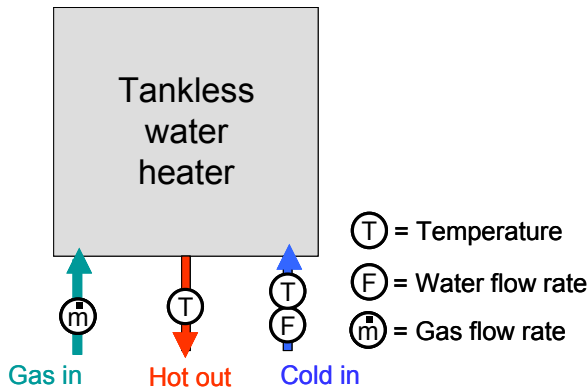


Fig. 5. Schematic of tankless water heater test setup (4).

Two data sets were used here, one for regression and one for validation. The data used for regression are shown in Fig. 6. The data contain periods with rise, steady-state, and decay of two types, as in Table IV. There is a fast decay at hour ~13.15 hr, when the burner was turned off while the draw at ~600 l/hr continued. The slow decay of T_{out} toward T_{env} at 13.22 hr is filled data. During steady-state, η_{burn} is the dominant parameter and UA losses can be estimated or neglected. During the rise and fast decay, C is the only unknown parameter of significance. Both UA and C are involved in the decay to T_{env} . dominant. Fig. 7 shows an independent set of validation data. This data consists of a sequence of draws with a delay of 10 min between each

draw; draw volume increases with each successive draw. By analyzing the steady portions during draw, the regression data showed $\eta_{burn} \sim 0.74 \pm 0.03$. The validation data showed $\eta_{burn} \sim 0.82 \pm 0.03$. The regression also indicated significantly different “best-fit” values for η_{burn} . It is unlikely that the difference between the two data sets is due to noise alone. Sources of this small discrepancy have not been identified.

4. DATA ANALYSIS

The key parameter values (η , C , UA) can be estimated by solving manually for parameters in discrete regions where their effect is dominant. Results are shown in Table 5. These values are useful as the starting points for the least squares search, and provide “sanity checks” for the more sophisticated but less intuitive regressions.

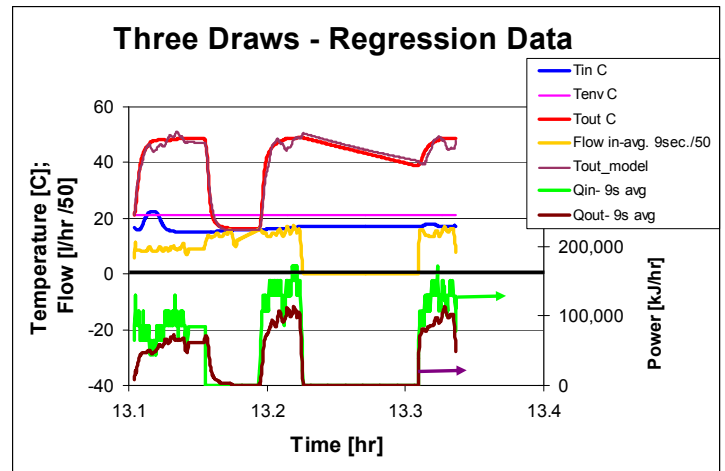


Fig. 6. TWH data used for regression of parameters.

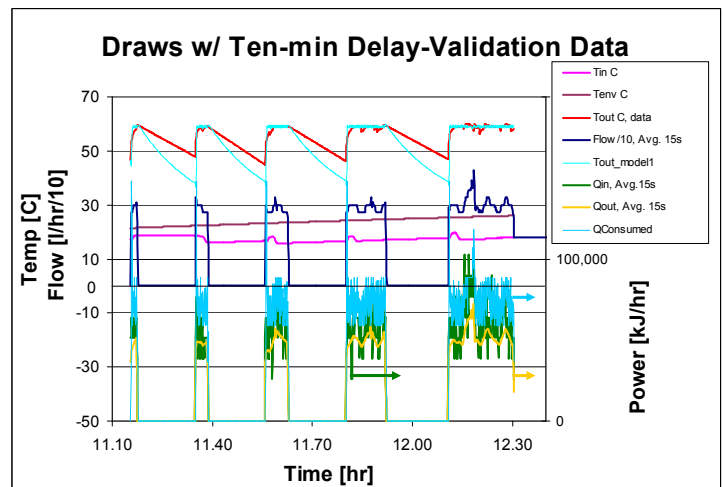


Fig. 7. Draws with 10 min delay between them. T_{out} varies about 2 °C in steady state; T_{out} variations are correlated with flow variations.

Least squares regression was done using the optimization routine GENOPT (6) to minimize a χ^2 metric:

$$\chi^2(\eta, C, UA) = \sum_i w_i [T_{out,data}(t_i) - T_{out,model}(t_i; \eta, C, UA)]^2_i \quad (2)$$

The weighting factor w_i is used to eliminate holes or otherwise weight χ^2 . For calibration runs, $m_{dot,in}(t_i)$, $T_{in}(t_i)$, $Q_{dot,in}(t_i)$, and $T_{env}(t_i)$ were inputs, and $T_{out}(t_i)$ was computed. The Hookes-Jeeves search method was used, and parameter values at the minimum are shown in Table 5. A number of variations on data sets, weighting methods, and constraints were done, with significant variations in parameters with these various assumptions. This indicates that the data are not well-conditioned for parameter regression. Results in Table 5 are considered a reasonable compromise.

TABLE 4. TANKLESS STATE AND EQUATION

Unit State	State Equation
Steady state ¹	$\eta Q_{dot,gas} = m_{dot} c_p (T - T_{in}) + UA(T - T_{env})$
Ramp-up ²	$CdT/dt = \eta Q_{dot,gas} - m_{dot} c_p (T - T_{in}) - UA(T - T_{env})$
Envir. decay ³	$CdT/dt = -UA(T - T_{env})$
Draw decay ⁴	$CdT/dt = -m_{dot} c_p (T - T_{in}) - UA(T - T_{env})$

1. Period when T_{out} is steady, within controller ability.
2. Period T start of draw up until steady state reached.
3. Mass temperature decay after firing; T_{out} approaches T_{env} .
4. Mass temperature decay after firing, but with the draw continuing; T_{out} approaches T_{in} .

A plot of χ^2 as a function of (C,UA) with η_{burn} fixed at the best estimate value (0.74) is shown in Fig. 8 for Fig. 6 data. The plot shows that the C value is fairly well determined, but the UA is not. C is well-determined because it is the only unknown in the first decay “with draw.” The second decay (to T_{env}) has UA and C equally involved, but the long decay is fill data and was not used, leaving insufficient weight in the data for UA. A manual estimate of 0.2 for the decay time constant in Fig. 6 was imposed to obtain an estimate of UA that fit the data in Fig. 6 reasonably well. Resulting parameter values are shown in Table 5. The modeled T_{out} is compared to measured values in Fig. 6. RMS deviation between modeled and measured outlet temperature was $\sim 1.7^\circ C$, not including the filled data. The calibrated model agreed very well with the data.

Table 5 shows two values for burner efficiency η_{burn} , corresponding to Fig. 6 and Fig. 7 data, respectively. It is expected from the manufacturer’s claims that η_{burn} would be about 82%. The value from regression on Fig. 6 data is about 11% lower. The regressed value from Fig. 7 data is 87%, some 6% higher. The thermal capacitance value is reasonably consistent with the water and metal in the heat exchanger. There is about 4 lbs of water and some 10 lbs in heat exchanger metal coupled to the water. This yield a capacitance estimate of $\sim 11 \text{ W}^\circ C$. The UA is very difficult

to estimate because of internal thermal shorts between the burner, heat exchanger, and supporting structure. However, the magnitude seems reasonable.

TABLE 5. PARAMETER ESTIMATES

Parameters	Burner Efficiency	Thermal Mass	Loss Coefficient
	%	kJ/°C	Watts/°C
Manual	74 ± 3^1 ; 81 ± 3^2	7 ± 3	10 ± 6
Least squares ³	73 ± 2^1 ; 87 ± 3^2	9.5 ± 2	13 ± 6^4

1. From Fig. 6 data.
2. From Fig. 7 data.
3. Regression result for Fig.6 data (except for 2nd value of η_{burn} , which was independently determined from Fig. 7 data.
4. Fixing the time constant allows determination of UA.

When model parameters are determined from one set of data, it is typical to validate the model by comparing it to an independent set of data. For validation in this study, Fig. 7 data were used. For these runs, $m_{dot,in}(t_i)$, $T_{in}(t_i)$, $T_{env}(t_i)$ and T_{set} were inputs, and $Q_{dot,in}(t_i)$ and $T_{out}(t_i)$ were computed. It can be seen that $T_{out,model}$ decays more rapidly than the data; the time constant appears too high, by about a factor of two. This may be due to error in estimating T_{env} . The simulation overpredicts the $Q_{in,gas}$ for the data set by $\sim 25\%$. This poor match indicates that the regressed burner efficiency of 73% from the calibration data set is significantly too low for the validation data set. It should be noted that when the 87% efficiency value is used, the model is in good agreement with the data. More data would be needed to resolve the efficiency problem, as it appears there is an internal inconsistency in the data. For resolving the decay problem, it is necessary to have measured values for T_{env} .

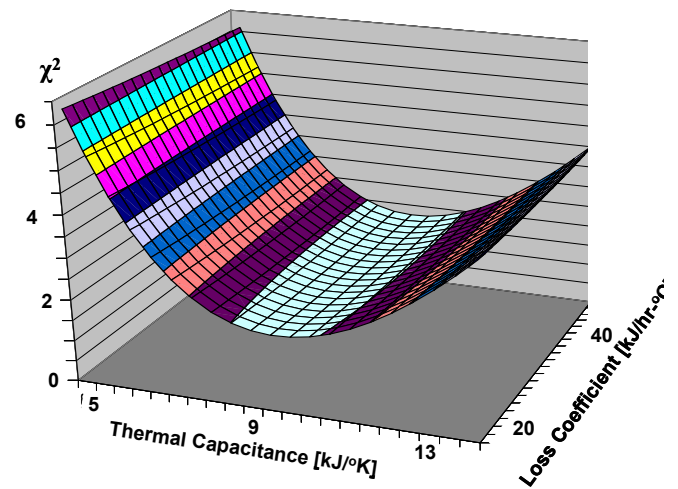


Fig. 8. A plot of χ^2 as a function of thermal capacitance C and loss coefficient UA, with η_{burn} fixed at the best-fit value.

5. APPLICATIONS OF THE MODEL

In this section, efficiency and stability questions are considered using the calibrated model.

5.1 Efficiency Calculation with Realistic Draws.

The baseline draw profile for the three-bedroom benchmark house in the *Building America Program* (7) was used as a representative realistic draw pattern (8). One day of this data is shown in Fig. 1. Over a year, the profiles are designed to match measured long-term time-of-use profiles and daily average volume for each end use. The key difference to the standard test draws is the presence of many small draws. To focus on variations solely due to draw differences, the model with efficiency set to 0.82 was run with the draw and other conditions specified for the standard test in (2). The resulting energy factor was 0.81. When the realistic draw was used, the efficiency was 0.74, reduced by about 8%. This result is consistent with the earlier empirical result in (3). It is clear that the result from standard tests (2) is inappropriate to use with realistic draws; rather, the procedure shown here should be used when accuracy better than 10% is desired for a realistic draw profile.

5.2 Addition of a Small Tank

TWH with feedback control have been reported to oscillate unstably if the Q_{dot} needed to reach setpoint is less than $Q_{dot,min}$ (3). Fig. 9 shows the domain in $(m_{dot}, \Delta T_{in})$ space where such oscillations are predicted to occur, for $Q_{dot,min} = 20$ kBtu/hr. Oscillations calculated by the current model are shown in Fig. 10. For these runs, T_{in} was varied sinusoidally to take the unit in and out of the unstable region. The potential for these large oscillations is likely the reason that most gas TWH manufacturers do not recommend using their units with a pre-heat system. It should be noted that these oscillations have not been well-reported in the open literature; evidence is only anecdotal, to our knowledge.

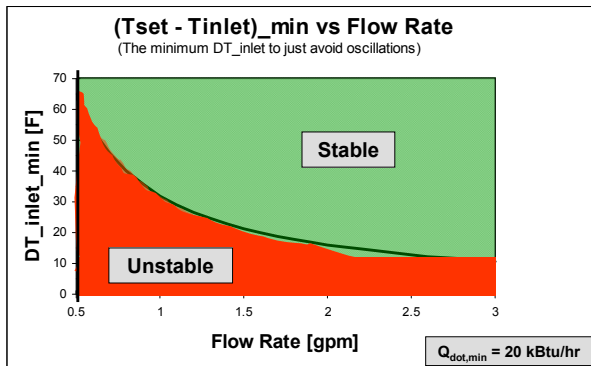


Fig. 9. Unstable/stable domains in $(m_{dot}, \Delta T_{in})$ space.

It is important to note that piping mass and mixing in the distribution system will reduce the magnitude of any such oscillations at the end-use point. Real distribution systems are relatively complex and piping lengths have increased significantly over the last several decades (9). Besides introducing delay in hot water delivery, the distribution system will damp out oscillations in the supply temperature. Complex flow patterns deviating from “plug flow” at low and high flows rates have been hypothesized that could also increase mixing (10). More work is needed to determine to what extent these mechanisms will reduce the oscillations at the end-use point.

It has been suggested (11) that a small storage tank be added, configured as shown in Fig. 11. Basically, the tank thermostat is used to activate the TWH loop to keep the tank at T_{set} , and draws occur through the (small) tank in the usual way, independent of the TWH loop. The flow rate in the pumped loop is several gpm, and $T_{set,tnkls}$ is set sufficiently high (e.g. 60 °C) that the TWH will always fire upon call for heat from the tank. Although it introduces added complexity and cost, this eliminates the limitations of low-flow cut-out and hot-water-out delay. Slow oscillations within the deadband of the tank thermostat now occur, depending on the tank volume, and mixing and stratification in the tank. An example is shown in Fig. 10; the TWH oscillated ~ 8 C, and the tank system ~ 2 C (the assumed tank deadband). The tank size and flow rate/pumping power in the tankless loop have not been optimized. If the tank is too small, the tankless will cycle too frequently. If the tank is too large, standby energy losses start to become significant, and the system efficiency significantly decreases.

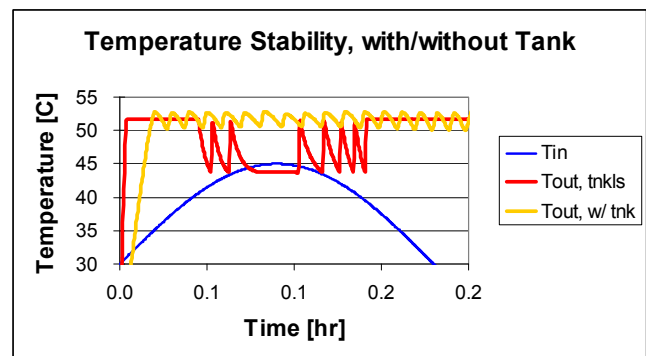


Fig. 10. Tankless oscillations as predicted by the model, with/without an added storage tank as shown in Fig. 11.

6. CONCLUSIONS

The efficiency of tankless water heaters depends significantly on the draw profile. Standard tests resulting in published energy factors (2) use large-volume draws only, 10.6 gal/draw. Although of no consequence for storage-tank

water heaters, this leads to an overestimate of the efficiency of tankless water heaters when a realistic draw pattern is used. A one-node thermal model was posed to facilitate accurate efficiency calculation. The key model parameters include burner efficiency, thermal mass, and loss coefficient to the environment sink. These parameters were determined from available test data taken for other purposes (3). The coupling to the environment was poorly estimated because data were not taken during decays, and because T_{env} was estimated, not measured. Nonetheless, the calibrated model matched the calibration data well.

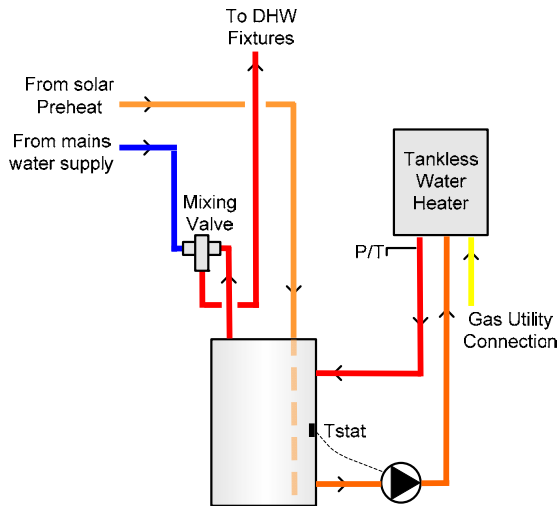


Fig. 11. Tankless water heater configured with a small tank to eliminate several issues with TWH (taken from [11]).

However, the calibrated model did not provide a good fit to an independent set of data; predicted Q_{in} was $\sim 25\%$ high. The model agreed with validation data reasonably well if the model burn efficiency was raised about 20%. The same conclusion is reached when comparing independent regressions on the two data sets. Efficiency was clearly inconsistent between the two data sets, whether as analyzed by the model or by hand calculations. The inconsistency between the two data sets was not resolved. Despite the inconsistency and uncertainty on efficiency, the model represents the data trends well and is viable to analyze problematic features of tankless.

The result of properly calculating efficiency was illustrated with a baseline draw profile from the *Building America Program* (7). Realistic draws show a high volume of small draws, which tend to lower the average efficiency of a tankless water heater. The realistic draw lowered efficiency by about 8% over the result from standard tests with large draws.

Data used here are not at all optimal for model studies, as they were designed for direct measurements of draw-

efficiency, not for parameter extraction (3). A test protocol will be developed that elicits stable, accurate values for parameters and addresses control questions.

7. NOMENCLATURE

Symbols

c_p	Heat capacity at constant pressure
C	Thermal capacity (water + heat exchanger)
DOE	Department of Energy
EF	Energy factor ($EF \equiv Q_{out}/Q_{in}$ @ 64 gal/day)
m_{dot}	mass flow rate
NREL	National Renewable Energy Laboratory
Q	Thermal energy
Q_{dot}	Thermal power
RMS	Root mean squared deviation
t	Time
T	Temperature
TWH	Tankless water heater
UA	Loss coefficient of the tankless water heater
χ^2	Metric of deviation between model and data
Δ	Difference

Subscripts

aux	Auxiliary input, fossil fuel or electrical
burn	Relating to the gas burner
data	Measured variable, from data
dband	Deadband for temperature control
deliv	Delivered to the hot water load
dot	Denotes the time derivative of m or Q
draw	Of or pertaining to a draw
env	Environment surrounding the tankless water heater
i	Index for data points or time-step
in	Incoming, either gas or water
load	Hot water load in the house
max	Maximum value
min	Minimum value
model	Computed model variable
needed	As needed to reach the setpoint
out	Outlet of the tankless water heater
set	Setpoint for outlet temperature
ss	Steady state
tank	Storage-tank water heater
tnkls	Tankless water heater

8. ACKNOWLEDGMENTS

The authors acknowledge funding from the U.S. Department of Energy, Office of Energy Efficiency and Renewable Energy, Buildings Technology Office. Support was provided by the *Building America Program* managed by Terry Logee, and by the *Solar Heating and Cooling Program* managed by Bob Hassett. Support and direction

from NREL DOE program managers Ren Anderson and Tim Merrigan is acknowledged.

9. REFERENCES

- (1) Davis Energy Group, “Residential Feasibility Assessment of Gas Tankless Water Heaters in PG&E Service Territory,” report to Pacific Gas and Electric Company, Application Assessment Report 0412
- (2) GAMA 2008. Gas Appliance Manufacturer’s Association. The tankless rating directory is accessible at <http://www.gamanet.org>. Links from that site take one to detailed description of the standard water heater test.
- (3) Davis Energy Group, *Field and Laboratory Testing of Tankless Gas Water Heater Performance*, report to PIER, April 2006. Available at PIER website.
- (4) TRNSYS, University of Wisconsin, Solar Energy Laboratory. Description can be found at: <http://sel.me.wisc.edu/trnsys/default.htm>
- (5) Technical Documentation Manual, TRNSYS Type 940 Gas Tankless Water Heater. TESS Component Libraries for TRNSYS 16, V2.1. Thermal Energy System Specialists (TESS) LLC, Madison WI 53719.
- (6) GENOPT. Description available at: <http://gundog.lbl.gov/GO.html>
- (7) *Building America Program*. See website at: http://www.eere.energy.gov/buildings/building_america/
- (8) Hendron, R., and J. Burch, “Development of Domestic Hot Water Event Schedules for Residential Buildings”, ASME ES2007, Long Beach, CA, June 2007.
- (9) Klein, G., “Hot Water Distribution Systems. Parts 1-3”, Plumbing Systems and Design, March-October 2004.
- (10) Hiller, C., “Hot water distribution system piping time, water, and energy waste - Phase I: Test results”, ASHRAE Transactions, v 112, 2006, p 415-425
- (11) Rudd, A., and H. Feldman, “Introducing the Market to High-performance Green Buildings on Hilton Head Island”, TO #KAAX-3-32443-15, 12/11/07. Available from A. Rudd at betsy@buildingscience.com

CP-1002: Preliminary Modeling, Testing and Analysis of a Gas Tankless Water Heater

About this Paper

This report was first presented at American Solar Energy Society Annual Conference, San Deigo, CA, May 2008.

About the Author

Armin Rudd is a principal engineer at Building Science Corporation in Somerville, Massachusetts. More information about Armin Rudd can be found at www.arminrudd.com.

Direct all correspondence to: Building Science Corporation, 30 Forest Street, Somerville, MA 02143.

Limits of Liability and Disclaimer of Warranty:

Building Science documents are intended for professionals. The author and the publisher of this article have used their best efforts to provide accurate and authoritative information in regard to the subject matter covered. The author and publisher make no warranty of any kind, expressed or implied, with regard to the information contained in this article.

The information presented in this article must be used with care by professionals who understand the implications of what they are doing. If professional advice or other expert assistance is required, the services of a competent professional shall be sought. The author and publisher shall not be liable in the event of incidental or consequential damages in connection with, or arising from, the use of the information contained within this Building Science document.